Desalination and Water Treatment
www.deswater.com
doi: 10.1080/19443994.2015.1130653

57 (2016) 21781–21793
October

Taylor & Francis
Taylor & Francis Group

Synthesis of coal cinder balls and its application for COD_{Cr} and ammonia nitrogen removal from aqueous solution

Yongmei Wang[a], Weijun Tian[a,b,*], Chenglin Wu[a], Jie Bai[a,b], Yangguo Zhao[a,b]

[a]*College of Environmental Science and Engineering, Ocean University of China, Qingdao 266100, P.R. China, email: yongmeiwang2011@163.com (Y. Wang), Tel. +86 532 66782356; Fax: +86 532 66782810; emails: weijunas@ouc.edu.cn (W. Tian), wucl1989@126.com (C. Wu), baijie@ouc.edu.cn (J. Bai), ygzhao@ouc.edu.cn (Y. Zhao)*
[b]*Key Laboratory of Marine Environmental Science and Ecology, Ministry of Education, Qingdao 266100, P.R. China*

Received 27 March 2015; Accepted 29 November 2015

ABSTRACT

A new adsorbing material, coal cinder ball, was synthesized, characterized, and applied to remove chemical oxygen demand (COD_{Cr}) and ammonia nitrogen (NH_4^+-N) from water. Since coal cinders contain harmful metals, the optimum pretreatment method was determined by testing the harmful metal concentrations of cinder leachate solution. The results demonstrated the optimum concentration of HCl in modified coal cinders was 6 mol/L. Due to large surface areas of modified coal cinders, they exhibited a high adsorption affinity for COD_{Cr} and NH_4^+-N. The adsorption kinetics of COD_{Cr} and NH_4^+-N on coal cinder balls could be expressed by the pseudo-second-order model, which revealed that the adsorption process consisted of physical adsorption and chemical adsorption. The adsorption isotherms were fitted well with the Langmuir isotherm, which might be due to homogenous distribution of active sites on the microspheres' surface. When the coal cinder balls were used to purify the micro-polluted river water, the removal of COD_{Cr} was much more than NH_4^+-N under different water volumes and packing lengths. When combined with zeolite at the ratio of 1:1, the removal rates of COD_{Cr} and NH_4^+-N increased significantly. This would overcome the shortcomings of zeolite single use and offer a wide application prospect in water treatment.

Keywords: Coal cinder ball; Adsorption; Zeolite; Micro-polluted water; COD_{Cr}; NH_4^+-N

1. Introduction

Coal is the main energy source in the world. Millions of tons of coal cinders as the products of coal combustion are discharged every year, but only 10% were reused in producing cement, power generation, and agricultural soil improvement [1,2]. Large numbers of coal cinders are piled on land for long time. The coal cinder piles do not only occupy large quantities of land, but also pollute the environment [3,4]. The effective reuse of coal cinders is an increasingly urgent concern worldwide.

In recent years, with the development of waste utilization technologies, coal cinders have been widely used as adsorbents to purify wastewater because of their honeycomb pores, large specific surface areas, and good permeability [5]. And some researches have begun to focus on how to improve the adsorption capacity of coal cinder, such as choosing different

*Corresponding author.

pretreatment conditions, coating the surface of honeycomb briquette cinders with iron, etc. [6–11]. These all provided prospective pathways for coal cinders utilization. However, earlier studies have demonstrated that coal cinders contained a large number of deleterious metals such as Al, Cr, Cu, As, Hg, Cd, and Pb [4]. When the coal cinders were placed directly into water to adsorb pollutants, harmful metals would be released into water body to cause the secondary pollution [12]. This limits the application of coal cinders. Meanwhile, in reuse process, coal cinders with low mechanical strength are easily broken [6,13], and then cause water turbidity and sedimentation blockage problems. The harmless treatment and mechanical strength improvement of coal cinders make them suitable for reuse in water treatment.

To expand the application of coal cinders, some harmless treatment ways of coal cinders from four coal districts in China were tried to determine the favorable pretreatment way. A construction method of cinder ball that could improve the mechanical strength was provided. In order to clarify the adsorption process of COD_{Cr} and NH_4^+-N, adsorption isotherms and kinetic studies were conducted in the synthetic wastewater containing potassium hydrogen phthalate (KHP) and NH_4Cl to provides the basis for COD and NH_4^+-N study [14]. The application of coal cinder balls combined with zeolite to purify actual micro-polluted river water was also studied.

2. Materials and methods

2.1. Raw material

Four coal cinders, obtained from Feicheng (Shandong province, China), Yuanbaoshan (Neimengu municipality, China), Nanpiao, and Qinghemen (Liaoning province, China), were dried in a drying closet for 24 h at 105°C for using. The chemical compositions of the four raw coal cinders were given in Table 1. Other chemicals were purchased from Beijing Chemical Reagents Company (Beijing, China) with at least analytical grade. Potassium hydrogen phthalate (KHP) and NH_4Cl were added to distilled water to adjust COD_{Cr} and NH_4^+-N concentration as the synthetic wastewater used in this study.

2.2. Preparation of coal cinder balls

Raw coal cinders (20 mesh) were pretreated with diluted HCl and H_2O_2. Ten grams of raw cinders were added to 100 mL of HCl, or HCl and H_2O_2 solution (1#, 4 mol/L HCl; 2#, 6 mol/L HCl; 3#, 7.2 mol/L HCl; 4#, 6 mol/L HCl and 0.05 mol/L H_2O_2; 5#, 6 mol/L HCl and 0.1 mol/L H_2O_2), respectively, and shaken by a horizontal oscillator for 8 h. After standing for 16 h, the liquid was then filtered. The modified cinders were repeatedly washed by distilled water until the pH of leaching liquid was 6.9–7, then dried in a closed container at room temperature for later use. Polyvinyl alcohol (PVA) was modified by succinic acid with the mass ratio of 5.6:1 at 85°C to improve the water resistance and adhesion [15–17]. Four modified cinder balls (A–D) with the diameter of 3 cm were prepared using 15 g modified coal cinders from four coal districts (Feicheng, Yuanbaoshan, Nanpiao, and Qinghemen) and 12 mL modified PVA in a balling plate, then dried at room temperature in a closed container.

2.3. Characterization of coal cinder balls

Raw and modified coal cinders were added to ultrapure water with a quantity–volume ratio of 1:10 and then shaken by a horizontal oscillator at 25°C for 8 h. The mixture was left to stand for 16 h and then filtered to detect the concentration of deleterious metals in the filtrates. After filtration, the remaining raw and modified coal cinders were dried at 40°C for 48 h in a closet for BET and SEM analysis. To detect the compressive strength, 30 g of modified coal cinders and 24 mL of modified PVA were placed into a cylinder (height, 4 cm; diameter, 5 cm). Zeta potentials were measured at different pH values using a Horiba SZ-100Z.

Table 1
Composition of cinders used %

Composition	SiO_2	Al_2O_3	TFe	TiO_2	CaO	MgO	CaF	MnO_2
Feicheng	41.54	33.15	6.21	1.45	0.49	0.44	ND	ND
Yuanbaoshan	60.77	18.15	4.88	0.33	1.05	1.85	0.28	0.73
Qinghemen	62.25	20.72	5.75	0.59	1.33	2.05	0.35	0.85
Nanpiao	65.17	19.68	4.97	0.61	1.24	2.15	0.39	0.74

2.4. Adsorption experiments

To determine the adsorption kinetics of coal cinder balls for COD_{Cr} and NH_4^+-N removal, batch experiments were performed in a series of 500-mL glass conical flasks. A total of 425 mg potassium hydrogen phthalate (KHP) was dissolved in distilled water and diluted to 1,000 ml, so this solution had a theoretical COD_{Cr} of 500 mg COD_{Cr}/L [18]. This solution was further diluted with distilled water to obtain the 50 mg COD_{Cr}/L. And the standard NH_4^+-N sample was prepared with a NH_4Cl concentration of 15 mg/L [19]. The initial pH of the water samples were adjusted using 0.1 mol/L NaOH or HCl. A total of 16 g cinder balls were added to 400 mL water samples and agitated in a shaker (XJ-III, Shaoguan Taihong medical instrument Co., Ltd, China) at 20˚C for 10, 20, 30, 60, 120, 180, and 240 min. Then the concentrations of KHP (COD_{Cr}) and NH_4^+-N left in the water samples were detected.

The adsorption isotherms were studied under the following process: The concentration of COD_{Cr} samples were prepared with KHP to 10, 20, 30, 40, and 50 mg COD_{Cr}/L. The concentration NH_4^+-N samples were prepared with NH_4Cl to 1, 2, 4, 8, 10, 20, and 40 mg/L. A total of 16 g cinder balls were added to 200 mL different KHP (COD_{Cr}) and NH_4^+-N samples, respectively. Then samples were shaken by a horizontal oscillator at 20˚C. At predetermined time, the concentrations of KHP (COD_{Cr}) and NH_4^+-N left in the water samples were analyzed. The trials were repeated three times for each sample. KHP (COD_{Cr}), NH_4^+-N adsorption capacity and percentage removal efficiency were calculated by Eqs. (1) and (2):

$$Q_t = \frac{(C_0 - C_t)V}{m} \quad (1)$$

$$\% \text{ Removal} = \frac{C_0 - C_t}{C_0} \times 100 \quad (2)$$

2.5. The application of coal cinder balls in micro-polluted river water

To study the absorption effect of coal cinder balls in micro-polluted river water, coal cinder balls and other absorbents were fastened in the experimental facilities (2 m × 0.5 m × 0.7 m, Fig. 1). The absorption efficiency of COD_{Cr} and NH_4^+ under different water volumes (0.9, 0.7, 0.5 m^3/h), packing lengths (1, 0.75, 0.5 m) and different combinations of absorbents (1:1, 2:1) were compared.

2.6. Analytical methods

Raw coal cinder and zeolite mineral contents were measured according to the standard method for silicon and organic matrix material (EPA3052, 1996). The concentrations of trace metal elements in cinder leaching solution were measured by inductively coupled plasma mass spectrometer (7500C, Agilent, America). The surface areas and interior structures were investigated by BET (ST-08A, Beijing analysis instrument factory, China) and SEM (S-4800, Hitachi, Japan). The compressive strength was tested by material test machine (YAW-300, Fangyuan experimental instrument Co., Ltd, China). COD_{Cr} concentration was measured though the rapid digested spectrophotometry method using potassium dichromate with a microware digestion system (XJ-III, Shaoguan Taihong medical instrument Co., Ltd, China). According to standard methods (Chinese HJ 535-2009), NH_4^+-N concentration was characterized though the Nessler's reagent spectrophotometric method using a spectrophotometer (752 SP, spectrumlab, China) at the wavelength of 420 nm.

3. Results and discussion

3.1. Pretreatment of coal cinders

To investigate the effect of different concentrations of HCl and H_2O_2 on treatment efficiencies of deleterious metals, the harmful metal concentrations in the different filtrates of raw cinder and modified cinder were shown in Fig. 2. The results showed that the concentrations of different harmful metals in filtrates of four coal cinders modified by five different ways changed significantly.

While the coal cinders from Feicheng were pretreated by five different combinations of HCl and H_2O_2, the concentration of Pb in filtrate changed slightly because of its low concentration (about 0.035 μg/L) in filtrate of raw coal cinders. However, the concentration of Pb in filtrate of other three kinds of coal cinders pretreated by HCl (4, 6, and 7.2 mol/L) decreased significantly, which is similar to other reports [20]. Compared to the three former pretreatment methods, the concentration of Pb in filtrate of Feicheng, Qinghemen and Nanpiao coal cinders increased more by the 4# and 5# pretreatment method. It can be attributed to the change in morphology of Pb induced by H_2O_2. So the 4# and 5# pretreatment method cannot be chosen as the best way.

Similar to the change in Pb, the concentration of Hg in filtrate of four kinds of coal cinders increased using the 4# and 5# pretreatment method. This is

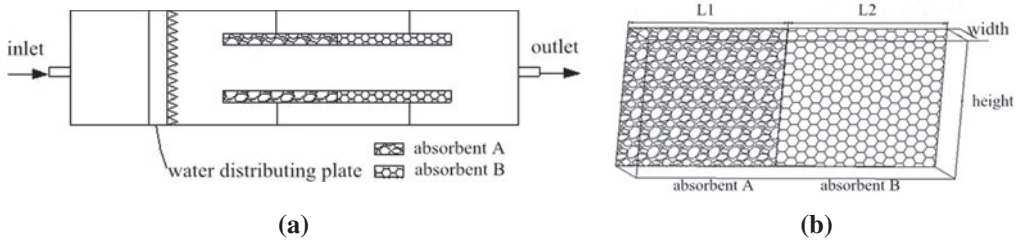

Fig. 1. Experimental facilities: (a) vertical view and (b) front view.

mainly because the morphology of Hg in the coal cinders was changed by H_2O_2, which was consistent with the reports of Martinez et al., Zhang et al. and Zhou et al. [21–23]. Meanwhile, it could be found that the concentration change in As, Cu, Cd, and Cr in filtrate of four kinds of coal cinders also was similar to the change in Pb and Hg as shown in Fig. 2.

Since the concentration of Al was the most among the different metals in the four kinds of coal cinders (Feicheng 33.15%, Yuanbaoshan 18.15%, Qinghemen 20.72%, Nanpiao 19.68%), the concentration of Al pretreated by HCl (4, 6, and 7.2 mol/L) in filtrate of four kinds of modified coal cinders decreased significantly. As can be seen in Fig. 2, the concentration of Al in the filtrate decreased with the increase in concentration of HCl. However, the concentration of Al in the filtrate of four different kinds of coal cinders increased under the 4# and 5# pretreatment method, which was similar to the change in the concentration of Hg, Pb, As, Cu, Cd, and Cr. So the cinders modified by 6 mol/L HCl were chosen in the study for high efficiency and low cost.

3.2. Characterization of coal cinder balls

The SEM images of four kinds of coal cinders before and after modification by 6 mol/L HCl are shown in Fig. 3. Fig. 3(A2, B2, C2, D2) showed that the surface was covered by numerous flake-like crystals after HCl treatment. It might be attributed to the conversion of water-soluble metals-containing compounds under the strong acidic condition.

The BET surface areas of the four kinds of coal cinders modified by 6 mol/L HCl were larger than the raw coal cinders as shown in Table 2. The surface areas of four kinds of modified coal cinders were 14.44–37.74 m^2/g, which were 1.23–2.07 times greater than the raw coal cinders (6.98–26.14 m^2/g).

The density of modified cinders (0.77–0.94 g/cm^3) was significantly lower than that of raw coal cinders (1.54–1.89 g/cm^3), suggesting that coal cinders modified in HCl could reduce the density of coal cinders as shown in Table 2. Therefore, cinder balls made of modified coal cinders could be easier to float in the water, and can increase the adsorption capacity of pollutants. All these were attributed to the use of 6 mol/L HCl, which could dissolve a large number of metals in coal cinders including Pb, Hg, Cd, As, Cu, Cr, and Al, thereby causing plenty of micropores and large surface areas.

Surface features and interior structure can reflect adsorption ability of material to some extent [24]. Since the larger surface areas the more adsorption capacity for some pollutants [19], the modified cinder balls could receive better removal efficiency for COD_{Cr} and NH_4^+-N.

The compressive strength of cinder balls was about 3.2–3.8 MPa, which was three times higher than the raw cinders (0.5–1.2 MPa) as shown in Table 2. Higher compressive strength could resist higher water pressure, and the coal cinder balls were unbroken. Therefore, coal cinder balls would be better to purify micro-polluted river water compared with the raw cinders directly used in the water treatment.

3.3. Influence of pH on adsorption of KHP (COD_{Cr}) and NH_4^+-N

The pH_{PZC} (point of zero charge) of coal cinder balls was calculated to be 6.0 according to the zeta potential shown in Fig. 4. When the reaction time was 240 min, the adsorption of KHP (COD_{Cr}) and NH_4^+-N on coal cinder balls was investigated at different pH values. As shown in Fig. 5, the highest treatment efficiencies were obtained at pH 6.0, removal efficiencies of KHP (COD_{Cr}) and NH_4^+-N were up to 40.7 and 25.2%, respectively. Charge conditions may influence the electrostatic force between solvated particle and the adsorbent. It is well known that a solid surface is positively charged when $pH < pH_{PZC}$, and negatively charged when $pH > pH_{PZC}$ [25]. Therefore, when pH was 3.0, the surface of coal cinder balls was positively charged, and the repulsion hindered the transferring of NH_4^+-N. The electrostatic repulsion decreased with

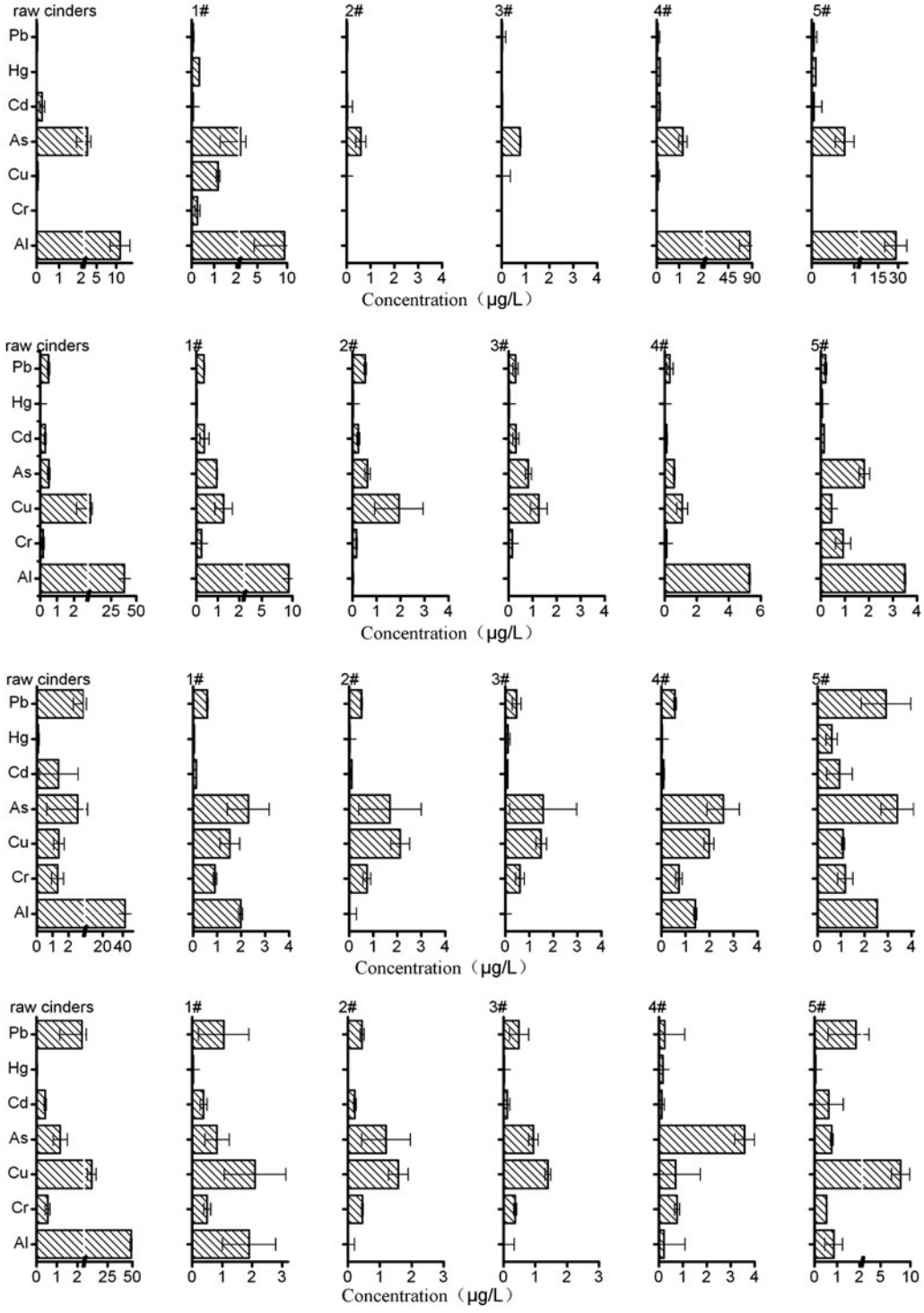

Fig. 2. Harmful metal concentration in filtrate of 4 kind of coal cinders (Feicheng, Yuanbaoshan, Nanpiao, Qinghemen; 1# 4 mol/L, 2# 6 mol/L, 3# 7.2 mol/L HCl, 4# 6 mol/L HCl and 0.05 mol/L H_2O_2, 5# 6 mol/L HCl and 0.1 mol/L H_2O_2).

the increase in pH. When pH > 6.0, electrostatic attraction and sorption happened simultaneously for NH_4^+-N removal. When pH > 8, NH_4^+ was gradually converted into the form of $NH_3{\cdot}H_2O$, which decreased the removal of NH_4^+-N. As for KHP (COD_{Cr}), when pH was 6.0 or lower than 6.0, electrostatic attraction

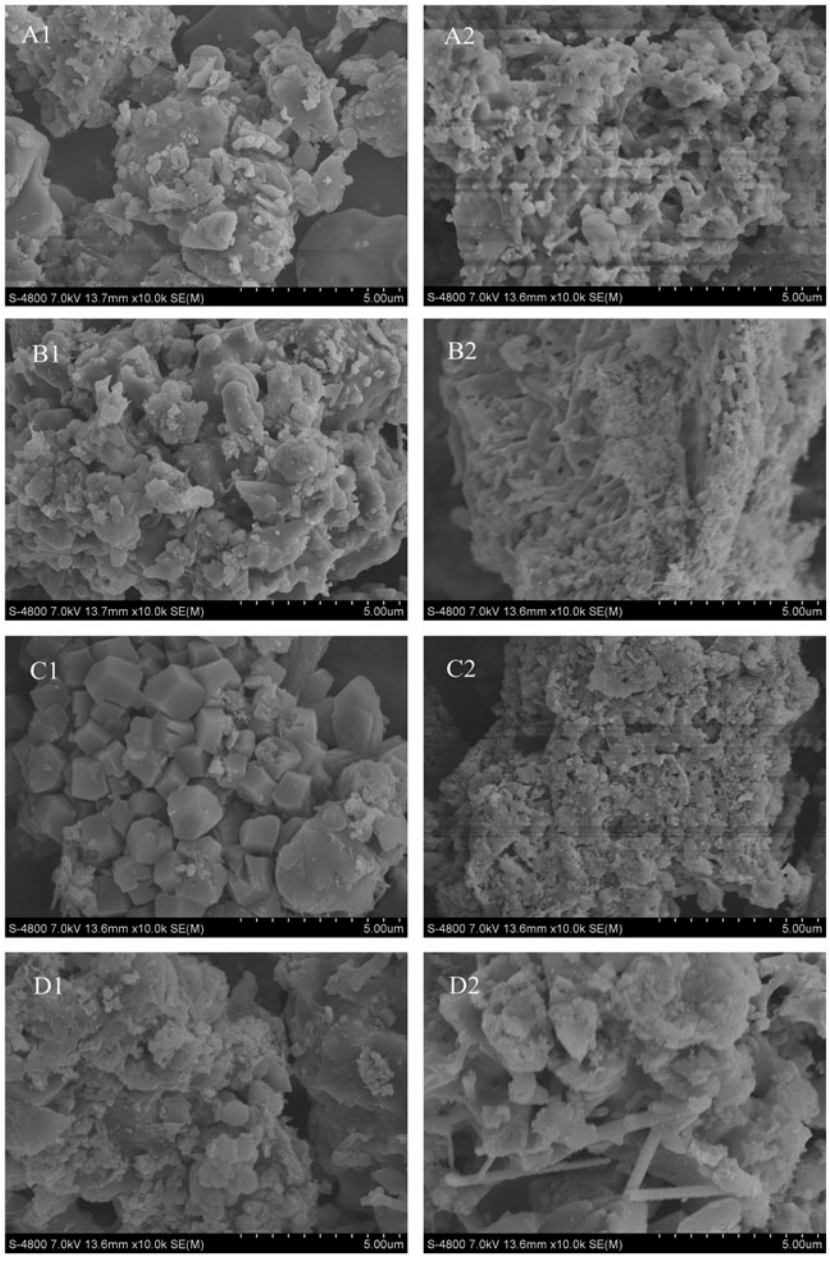

Fig. 3. SEM of four kinds of coal cinders (Feicheng, Yuanbaoshan, Nanpiao, Qinghemen) before modification (A1–D1) and after modification (A2–D2).

Table 2
Parameters of coal cinders before and after modification

	Feicheng		Yuanbaoshan		Nanpiao		Qinghemen	
Indicator	Before	After	Before	After	Before	After	Before	After
BET (m^2/g)	6.98	14.44	24.20	27.25	13.51	22.14	26.14	37.74
Packing density (g/cm^3)	1.81	0.92	1.54	0.77	1.89	0.94	1.85	0.93
Compressive strength (MPa)	1.2	3.8	0.7	3.5	0.9	3.6	0.5	3.2

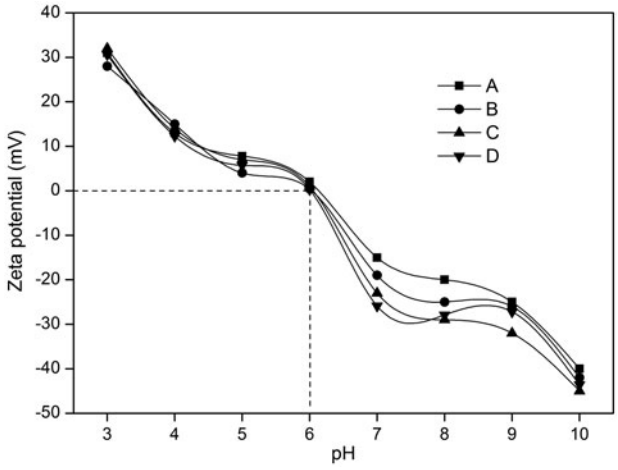

Fig. 4. Zeta potential of coal cinder balls.

promoted the KHP (COD_{Cr}) removal. When pH > 6.0, the repulsion hindered the transferring of KHP (COD_{Cr}). Therefore, pH 6.0 was chosen as the optimal pH.

3.4. Adsorption kinetics

Numerous adsorption processes have been investigated particularly during the past 25 years [26–31]. It has been known that adsorption processes could be dependent on and controlled by different kinds of mechanisms, such as diffusion control, mass transfer, chemical reactions, and particle diffusion. As shown in Fig. 6, the adsorption of KHP (COD_{Cr}) and NH_4^+-N onto four kinds of coal cinder balls was initially fast and then gradually slowed. When reaction time increased to 120 min, the KHP (COD_{Cr}) adsorption capacity of cinder ball C achieved to 0.24 mg/g with a removal efficiency of 32.3%. KHP (COD_{Cr}) adsorption capacity increased slightly when reaction time was increased from 120 to 240 min. It might be deduced that the adsorption of KHP (COD_{Cr}) on cinder ball C reached equilibrium at 120 min, which is less than three other cinder balls (180 min). As for NH_4^+-N, the adsorption equilibrium of four cinder balls all reached when the reaction time was 120 min. And the adsorption amount of cinder ball A was up to 0.09 mg/g with the removal rate of 26%, significantly higher than the others. This might be attributed to higher contents of the total Fe (TFe) in cinder ball A, which could increase the theoretical nitrogen saturation amount [17].

The pseudo-first-order kinetic model of Lagergren followed by Eq. (3) [32] and the pseudo-second-order kinetics equation followed by Eq. (4) [33,34] was used to illustrate the adsorption capacity of four kinds of cinder balls on KHP (COD_{Cr}) and NH_4^+-N.

$$\ln(Q_e - Q_t) = \ln Q_e - K_1 t \tag{3}$$

$$\frac{t}{Q_t} = \frac{1}{Q_e} t + \frac{1}{K_2 Q_e^2} \tag{4}$$

The best fit model was selected based on both the correlation coefficient (r^2) and the calculated Q_e values.

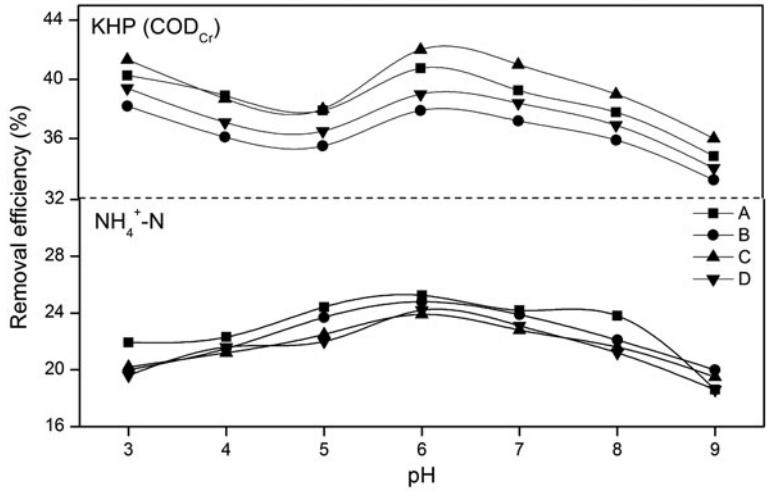

Fig. 5. pH effect on KHP (COD_{Cr}) and NH_4^+-N removal efficiencies, respectively.

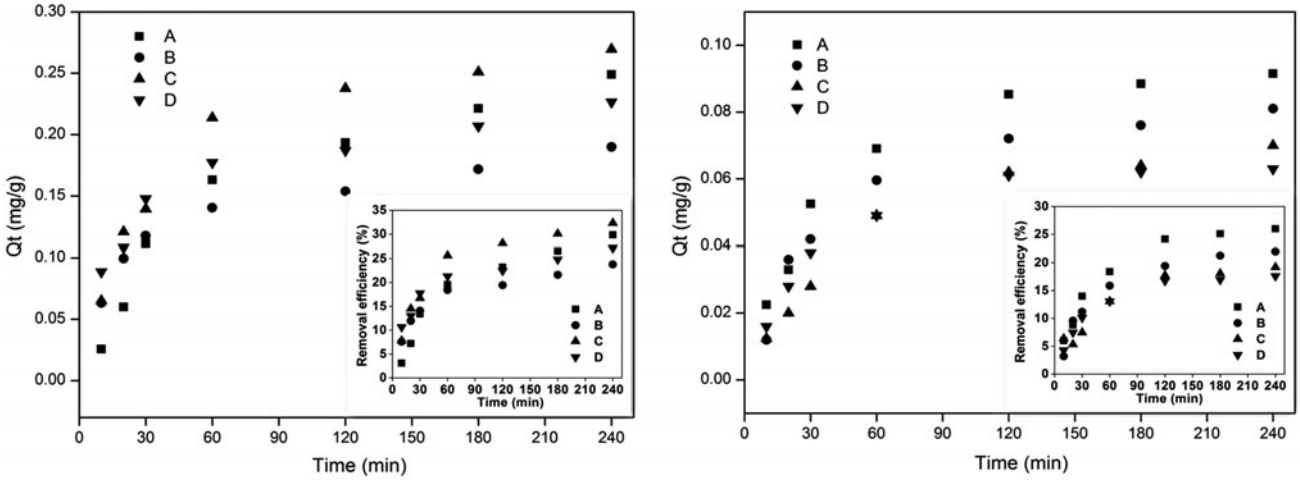

Fig. 6. Adsorption kinetics of KHP (COD_{Cr}) and NH_4^+-N on coal cinder balls, respectively.

The values of the function and parameters (Q_e, K_1, K_2) and the related correlation coefficients (r^2 values) of the four cinder balls were, respectively, calculated from the linear plot of $\log(Q_e - Q_t)$ vs. t in pseudo-first-order model and linear plot of t/Q_t vs. t for pseudo-second-order model. Table 3 showed that the pseudo-second-order kinetics model provided a near perfect match between the theoretical and experimental data (all greater than 0.9751 for r^2). So it could be concluded that the removal mechanisms of KHP (COD_{Cr}) and NH_4^+-N contained not only physical adsorption but also chemical adsorption.

3.5. Adsorption isotherms

Equilibrium data, commonly known as adsorption isotherms, are basic requirements for the research of adsorption systems [35]. The adsorption isotherms are important for the description of the equilibrium relationship between adsorbent and adsorbate. Adsorption of pollutants from liquid solution by solid adsorbents was widely evaluated using the Langmuir isotherm model followed by Eq. (5) [33,34] and Freundlich isotherm followed by Eq. (6) [36]:

Table 3
Parameters obtained from pseudo-first-order kinetics model, pseudo-second-order kinetics model, Langmuir, and Freundlich adsorption isotherms for four coal cinder balls

		COD adsorbtion				NH_4^+-N adsorbtion			
Models	Parameters	Ball A	Ball B	Ball C	Ball D	Ball A	Ball B	Ball C	Ball D
Pseudo-first-order kinetics model	Q_e	0.0598	0.0382	0.0349	0.0307	0.2339	0.1716	0.2609	0.2049
	K_1	0.0229	0.0264	0.0153	0.0282	0.0172	0.0411	0.0280	0.0418
	r^2	0.9284	0.9133	0.9800	0.9519	0.9502	0.9307	0.9899	0.9016
Pseudo-second-order kinetics equation	Q_e	0.2920	0.2000	0.2390	0.3050	0.0750	0.0470	0.0370	0.0450
	K_2	0.0619	0.2205	0.1903	0.1026	0.2979	0.5865	0.7639	0.3167
	r^2	0.9751	0.9925	0.9941	0.9965	0.9890	0.9916	0.9963	0.9949
Langmuir adsorption isotherm	Q_m	0.3400	0.4300	0.4400	0.4000	0.1100	0.1400	0.1200	0.1100
	b	0.0998	0.0263	0.0343	0.0756	0.1676	0.1063	0.0167	0.0398
	r^2	0.9988	0.9904	0.9953	0.9996	0.9922	0.991	0.99	0.9932
Freundlich isotherm	n	1.9159	1.4466	1.5518	1.6902	1.2017	1.2474	0.8651	1.0160
	K_F	0.0459	0.0183	0.0249	0.0393	0.0153	0.0131	0.0016	0.0038
	r^2	0.9336	0.9667	0.9593	0.9680	0.9704	0.9977	0.9689	0.9783

$$\frac{1}{Q_e} = \frac{1}{bQ_m}\frac{1}{C_e} + \frac{1}{Q_m} \quad (5)$$

$$Q_e = K_F C_e^{1/n} \quad (6)$$

The isotherms of KHP (COD_{Cr}) and NH_4^+-N adsorption by cinder balls were shown in Fig. 7 and Table 3. Table 3 showed that the Langmuir adsorption isotherms equation represented the better fit of experimental data due to the relatively better r^2 values (all greater than 0.9900 for r^2) compared with that of the Freundlich isotherm equation. This might be due to homogenous distribution of active sites on the microspheres surface since the Langmuir equation assumes that the surface was homogeneous and adsorption was a monolayer reaction [37]. So it could be seen that the absorption of KHP (COD_{Cr}) and NH_4^+-N on cinder balls was in monomolecular type.

The results showed that the theoretical KHP (COD_{Cr}) saturation amount (Q_m) of cinder ball C obtained from Langmuir model was the highest (0.44 mg/g) because of the largest BET surface area providing more adsorption sites [33]. Meanwhile, the theoretical KHP (COD_{Cr}) saturation amount of cinder ball A was the least (0.34 mg/g), because the BET surface area of cinder ball A was the least among the four kinds of cinder balls. Although the BET surface areas of the four cinder balls are different, the theoretical NH_4^+-N saturation amounts of the four cinder balls were very similar (0.11–0.14 mg/g). The reason for this similarity might be that the removal mechanisms of NH_4^+-N were physical and chemical adsorptions [19].

3.6. Application study of coal cinder balls in micro-polluted river water

Since the KHP (COD_{Cr}) and NH_4^+-N could be removed from aqueous solution by coal cinder balls, the efficiency of coal cinder balls on COD_{Cr} and NH_4^+-N in micro-polluted river water was studied for researching the adsorption capacity further.

3.6.1. Effect of different water volumes on removal efficiency

Fig. 8 shows that the removal efficiency of COD_{Cr} and NH_4^+-N under different water volumes when the packing lengths of coal cinders was 1 m. It could be concluded that the removal efficiency of COD_{Cr} increased with the decrease in inflow volume. The average removal efficiency was 21.7% when the inflow was 0.5 m^3/h, the average removal efficiency was 17% when the inflow was 0.9 m^3/h. Considering the different water volumes, the average removal efficiency of COD_{Cr} was the highest when the water volume was 0.9 m^3/h. Under different water volumes, the removal efficiency of NH_4^+-N was 12.3, 13.1, and 15.4%, respectively. Overall, using coal cinder balls, we can see that the COD_{Cr} removal efficiency was higher than the removal efficiency of NH_4^+-N obviously.

3.6.2. Effect of different packing lengths on removal efficiency

The effect of different packing lengths on removal efficiency of coal cinder balls under the condition of 0.9 m^3/h water volumes was shown in Fig. 9. As shown in Fig. 7, the removal efficiency of COD_{Cr} of

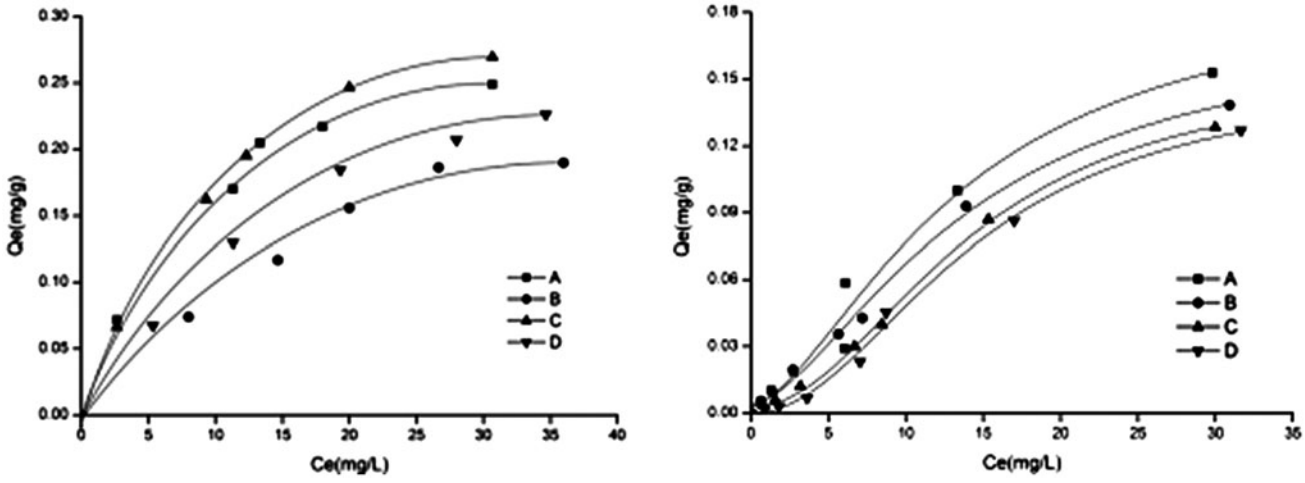

Fig. 7. Adsorption isotherms of KHP (COD_{Cr}) and NH_4^+-N on coal cinder balls, respectively.

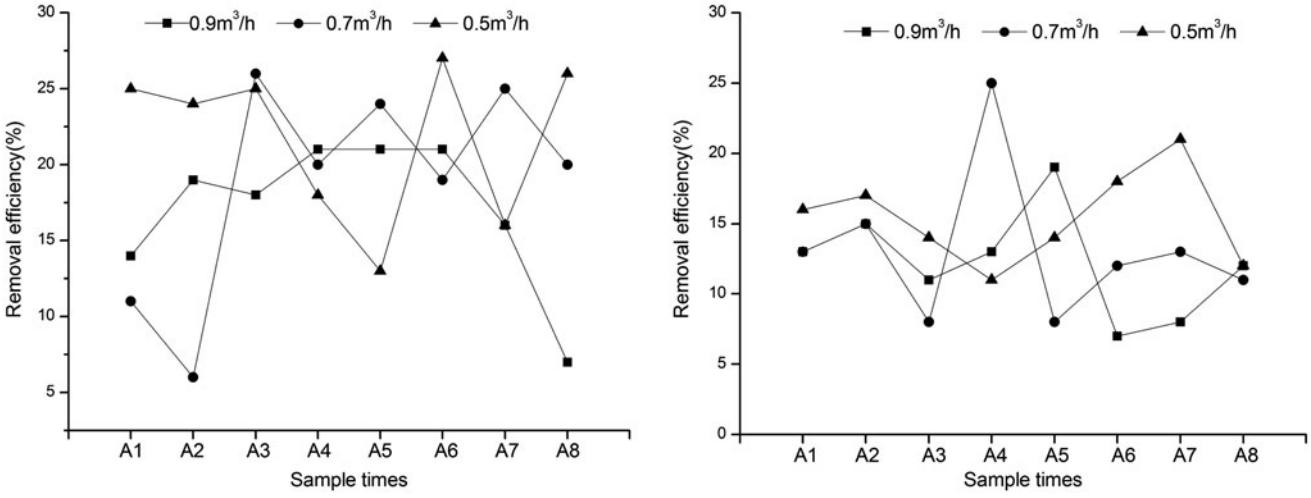

Fig. 8. Removal efficiency of COD and NH_4^+-N about coal cinder balls under different water volumes.

1 m packing lengths was 17%, which was more than the other two packing length. Similar to the removal efficiency of COD_{Cr}, the removal efficiency of NH_4^+-N of 1 m packing length was 12.3%, which was 1.5 times more than the removal efficiency of 0.5 m packing length. So the 1 m packing length was the optimal length to purify the micro-polluted river water.

3.6.3. Effect of combinations with coal cinder balls and zeolite on removal efficiency

Based on the above analysis, the removal efficiency of NH_4^+-N was lower when only coal cinder balls were used. So it was necessary to improve adsorption capacity of coal cinder balls in NH_4^+-N. Zeolite, as an effective adsorbent, is considered to be one of the most widely used adsorbent material. Zeolite could adsorb large quantity of NH_4^+-N in aqueous solution, however, the purification for COD_{Cr} was not significance [38]. So optimal combinations with coal cinder balls and zeolite was studied to purify micro-polluted river water more efficiently.

The removal efficiency of COD_{Cr} and NH_4^+-N under different combinations was shown in Fig. 10. Fig. 10 showed that COD_{Cr} removal efficiency of two different combinations were all up to 20% when the water volumes was 0.9 m^3/h, which was higher than the removal efficiency of zeolite. The NH_4^+-N removal efficiency of the combinations (2:1) was 11.8%, which

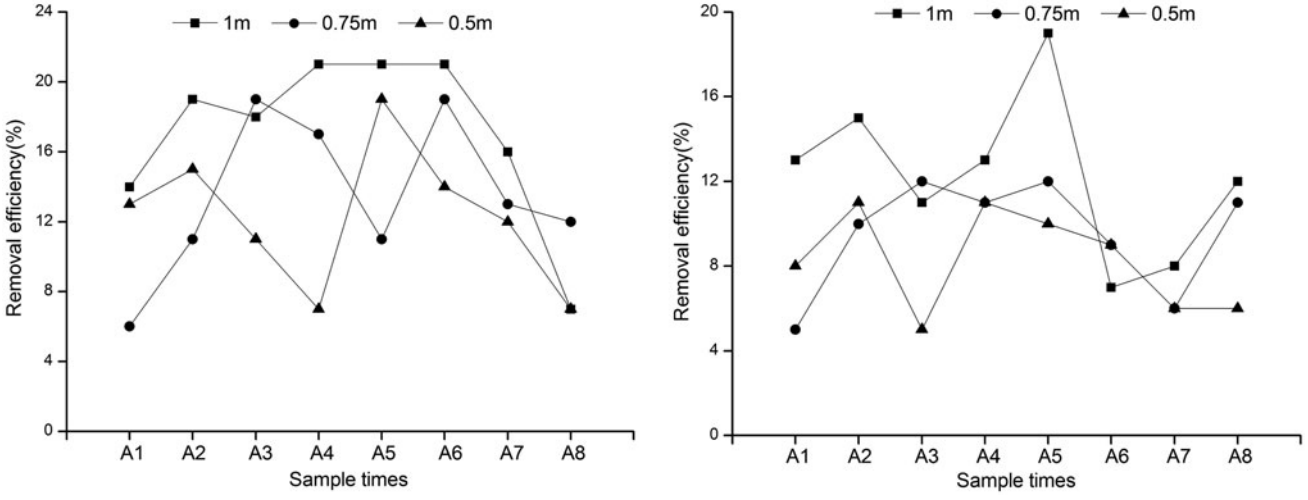

Fig. 9. Removal efficiency of COD and NH_4^+-N about coal cinder balls under different packing lengths.

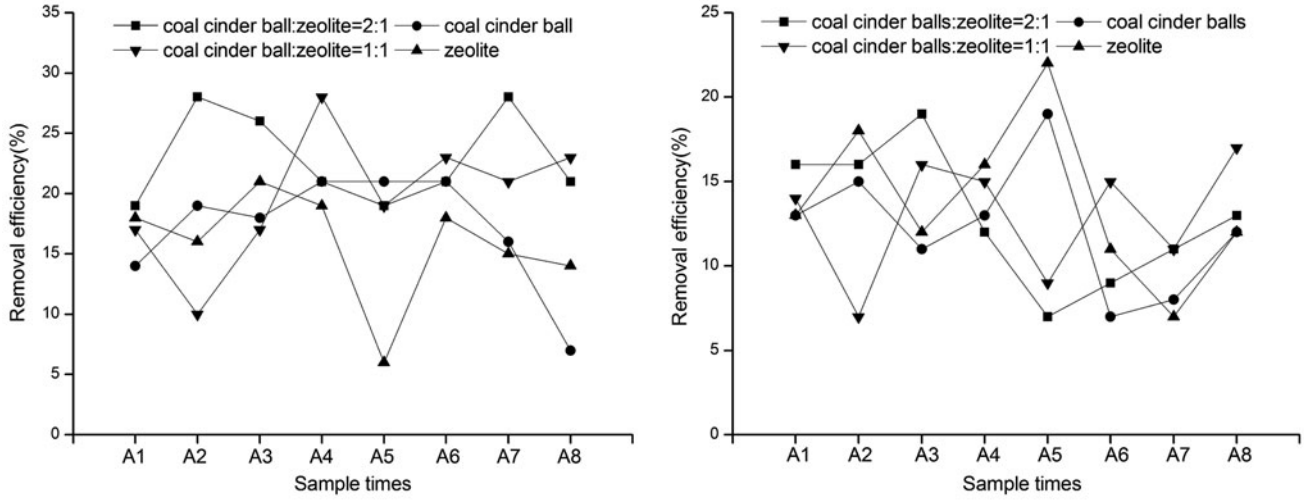

Fig. 10. Removal efficiency of COD and NH_4^+-N under different combinations.

was less than the removal efficiency of the combinations (1:1, 12.9%). It could be attributed to the improvement of zeolite to the adsorption of NH_4^+-N. It was visible that coal cinder balls as a kind of new packing could adsorb COD_{Cr} and NH_4^+-N obviously in aqueous solution, and the combinations with coal cinder balls and zeolite could overcome the shortcomings of zeolite to expand its wider application in water purification.

4. Conclusions

Cinder balls were successfully prepared by modified coal cinders and organic binder (PVA) and applied for the removal of COD_{Cr} and NH_4^+-N. When the coal cinders were modified by 6 mol/L HCl, the concentrations of harmful metals in coal cinders decreased and the adsorption capacity increased. Combination of coal cinder balls and zeolite was used to purify the micro-polluted river water. The different combinations of coal cinder balls and zeolite could improve the adsorption of COD_{Cr} and NH_4^+-N, which could expand more application in purification of the micro-polluted surface water.

Acknowledgments

This work was supported by the 12th Five-Year Plan of National Science and Technology Support (No. 2015BAB07B02) and National Water Pollution Control and Management Technology Major Project of China (No. 2013ZX07202-007). The authors would like to thank the anonymous reviewers for their recommendations and comments.

List of symbols

- Q_t — adsorption capacity of COD_{Cr} and NH_4^+-N at time t (mg/g)
- C_0 — the initial concentrations of COD_{Cr} and NH_4^+-N in the solution (mg/L)
- C_t — the final concentrations of COD_{Cr} and NH_4^+-N in the solution (mg/L)
- V — the solution volume (mL)
- m — the mass of cinder balls (g)
- t — the adsorption time (min)
- K_2 — the second-order reaction constant (g/mg min)
- Q_e — adsorption capacity of COD_{Cr} and NH_4^+-N at equilibrium (mg/g)
- Q_m — the theoretical amount required for adsorption saturation (mg/g)
- C_e — the solution concentration at equilibrium (mg/L)
- b — a constant
- $1/n$ — a constant
- K_F — a constant

References

[1] M. Singh, R. Siddique, Effect of coal bottom ash as partial replacement of sand on properties of concrete, Resour. Conserv. Recy. 72 (2013) 20–32.
[2] R. Kikuchi, Application of coal ash to environmental improvement, Resour. Conserv. Recy. 27 (1999) 333–346.
[3] G. Fellet, L. Marchiol, D. Perosa, G. Zerbi, The application of phytoremediation technology in a soil contaminated by pyrite cinders, Ecol. Eng. 31 (2007) 207–214.
[4] L. Zhang, H. Zhang, W. Guo, Y. Tian, Sorption characteristics and mechanisms of ammonium by coal by-products: Slag, honeycomb-cinder and coal gangue, Int. J. Environ. Sci. Technol. 10 (2013) 1309–1318.

[5] X. Yue, X. Li, D. Wang, T. Shen, X. Liu, Q. Yang, G. Zeng, D. Liao, Simultaneous phosphate and CODcr removals for landfill leachate using modified honeycomb cinders as an adsorbent, J. Hazard. Mater. 190 (2011) 553–558.
[6] J. Yang, S. Wang, Z. Lu, J. Yang, Converter slag-coal cinder columns for the removal of phosphorous and other pollutants, J. Hazard. Mater. 168 (2009) 331–337.
[7] S. Wang, J. Yang, S. Lou, Wastewater treatment performance of a vermifilter enhancement by a converter slag-coal cinder filter, Ecol. Eng. 36 (2010) 489–494.
[8] T. Sheng, S.A. Baig, Y. Hu, X. Xue, X. Xu, Development, characterization and evaluation of iron-coated honeycomb briquette cinders for the removal of As(V) from aqueous solutions, Arabian J. Chem. 7 (2014) 27–36.
[9] S.A. Baig, J. Zhu, L. Tan, X. Xue, C. Sun, X. Xu, Influence of calcination on magnetic honeycomb briquette cinders composite for the adsorptive removal of As (III) in fixed-bed column, Chem. Eng. J. 257 (2014) 1–9.
[10] J. Yu, W. Liang, L. Wang, F. Li, Y. Zou, H. Wang, Phosphate removal from domestic wastewater using thermally modified steel slag, J. Environ. Sci. 31 (2015) 81–88.
[11] J. Zhu, S.A. Baig, T. Sheng, Z. Lou, Z. Wang, X. Xu, Fe_3O_4 and MnO_2 assembled on honeycomb briquette cinders (HBC) for arsenic removal from aqueous solutions, J. Hazard. Mater. 286 (2015) 220–228.
[12] R.K. Singh, N.C. Gupta, B.K. Guha, The leaching characteristics of trace elements in coal fly ash and an ash disposal system of thermal power plants, Energy Sources Part A 34 (2012) 602–608.
[13] M. Singh, R. Siddique, Strength properties and microstructural properties of concrete containing coal bottom ash as partial replacement of fine aggregate, Constr. Build. Mater. 50 (2014) 246–256.
[14] Y.H. Han, Q. Cheng, J.Q. Chen, C.H. Zhou, H.M. Zhang, S.Q. Zhang, H.J. Zhao, Extending the photoelectrocatalytic detection range of KHP by eliminating self-inhibition at TiO_2 nanoparticle electrodes, J. Electroanal. Chem. 738 (2015) 209–216.
[15] G. Zhou, Z. Wang, W. Li, Q. Yao, D. Zhang, Graphene-oxide modified polyvinyl-alcohol as microbial carrier to improve high salt wastewater treatment, Mater. Lett. 156 (2015) 205–208.
[16] R. Hou, L. Nie, G. Du, X. Xiong, J. Fu, Natural polysaccharides promote chondrocyte adhesion and proliferation on magnetic nanoparticle/PVA composite hydrogels, Colloids Surf., B 132 (2015) 146–154.
[17] Z. Majidnia, A. Idris, Efficiency of barium removal from radioactive waste water using the combination of maghemite and titania nanoparticles in PVA and alginate beads, Appl. Radiat. Isot. 105 (2015) 105–113.
[18] I. Vyrides, D.C. Stuckey, A modified method for the determination of chemical oxygen demand (COD) for samples with high salinity and low organics, Bioresour. Technol. 100 (2009) 979–982.
[19] G. Ji, Y. Zhou, J. Tong, Nitrogen and phosphorus adsorption behavior of ceramsite material made from coal ash and metallic iron, Environ. Eng. Sci. 27 (2010) 871–878.
[20] E.E.V. Chapman, G. Dave, J.D. Murimboh, A review of metal (Pb and Zn) sensitive and pH tolerant bioassay organisms for risk screening of metal-contaminated acidic soils, Environ. Pollut. 179 (2013) 326–342.
[21] A.I. Martinez, B.K. Deshpande, Kinetic modeling of H_2O_2-enhanced oxidation of flue gas elemental mercury, Fuel Process. Technol. 88 (2007) 982–987.
[22] A. Zhang, Y. Li, Removal of phenolic endocrine disrupting compounds from waste activated sludge using UV, H_2O_2 and UV/H_2O_2 oxidation processes: Effects of reaction conditions and sludge matrix, Sci. Total Environ. 493 (2014) 307–323.
[23] C. Zhou, L. Sun, A. Zhang, C. Ma, B. Wang, J. Yu, S. Su, S. Hu, J. Xiang, Elemental mercury (Hg^0) removal from containing SO_2/NO flue gas by magnetically separable $Fe_{2.45}Ti_{0.55}O_4/H_2O_2$ advanced oxidation processes, Chem. Eng. J. 273 (2015) 381–389.
[24] M. Hartman, O. Trnka, M. Pohořelý, Minimum and terminal velocities in fluidization of particulate ceramsite at ambient and elevated temperature. Ind. Eng. Chem. Res. 46 (2007) 7260–7266.
[25] M. Xing, L.J. Xu, J.L. Wang, Mechanism of Co(II) adsorption by zero valent iron/graphene nanocomposite, J. Hazard. Mater. 301 (2016) 286–296.
[26] A. Kara, B. Osman, A. Göçenoğlu, N. Beşirli, Kinetic, isothermal, and thermodynamic studies of Cr(VI) adsorption on L-tryptophan-containing microspheres, Environ. Eng. Sci. 31 (2014) 261–271.
[27] X. Liu, Y. Li, C. Wang, M. Ji, Comparison study on Cr (VI) removal by anion exchange resins of Amberlite IRA96, D301R, and DEX-Cr: Isotherm, kinetics, thermodynamics, and regeneration studies, Desalin. Water Treat. 55 (2015) 1840–1850.
[28] H.N. Bhatti, S. Nausheen, Equilibrium and kinetic modeling for the removal of Turquoise Blue PG dye from aqueous solution by a low-cost agro waste, Desalin. Water Treat. 55 (2015) 1934–1944.
[29] B. Oliver-Rodríguez, A. Zafra-Gómez, M.S. Reis, B.P.M. Duarte, C. Verge, J.A. de Ferrer, M. Pérez-Pascual, J.L. Vílchez, Wide-range and accurate modeling of linear alkylbenzene sulfonate (LAS) adsorption/desorption on agricultural soil, Chemosphere 138 (2015) 148–155.
[30] P. Iovino, S. Canzano, S. Capasso, A. Erto, D. Musmarra, A modeling analysis for the assessment of ibuprofen adsorption mechanism onto activated carbons, Chem. Eng. J. 277 (2015) 360–367.
[31] G. Yang, Y. Liu, S. Song, Competitive adsorption of As(V) with co-existing ions on porous hematite in aqueous solutions, J. Environ. Chem. Eng. 3 (2015) 1497–1503.
[32] R.L. Tseng, F.C. Wu, R.S. Juang, Characteristics and applications of the Lagergren's first-order equation for adsorption kinetics, J. Taiwan Inst. Chem. Eng. 41 (2010) 661–669.
[33] M. Özacar, Equilibrium and kinetic modeling of adsorption of phosphorus on calcined alunite, Adsorption 9 (2003) 125–132.
[34] B. Kostura, H. Kulveitová, J. Leško, Blast furnace slags as sorbents of phosphate from water solutions, Water Res. 39 (2005) 1795–1802.

[35] E. Bulut, M. Özacar, İ.A. Şengil, Equilibrium and kinetic data and process design for adsorption of Congo Red onto bentonite, J. Hazard. Mater. 154 (2008) 613–622.
[36] Y. Yan, X. Sun, F. Ma, J. Li, J. Shen, W. Han, X. Liu, L. Wang, Removal of phosphate from wastewater using alkaline residue, J. Environ. Sci. 26 (2014) 970–980.
[37] M. Doğan, M. Alkan, Ö. Demirbaş, Y. Özdemir, C. Özmetin, Adsorption kinetics of maxilon blue GRL onto sepiolite from aqueous solutions, Chem. Eng. J. 124 (2006) 89–101.
[38] A.M. Cardoso, A. Paprocki, L.S. Ferret, C.M.N. Azevedo, M. Pires, Synthesis of zeolite Na-P1 under mild conditions using Brazilian coal fly ash and its application in wastewater treatment, Fuel 139 (2015) 59–67.